

VALIDATION OF A SIMPLIFIED MODEL FOR THE DESIGN OF MASONRY INFILLED FRAMES

Paulo B. Lourenço¹, Rita C. Alvarenga², Roberto M. Silva³

Abstract

The design of masonry infills is an issue that has attracted the attention of several researchers in the past, both from the experimental and analytical points of view. Nevertheless, the results are often questionable due to the large variability of masonry properties, the limited number of tests carried out and the large number of influencing factors. This paper addresses this limitation by using numerical analysis as a simulation of an experimental laboratory, and by performing a sensitivity analysis about the influence of the different influence factors. The modelling approach has been validated using the experimental results of two masonry walls subjected to horizontal loading. The parametric study subsequently carried out allowed to propose a strut-and-tie model that provides a novel simplified expression for the failure of infill walls belonging to frames subjected to horizontal loading. The proposed model is compared with other models available in the literature exhibiting superior performance and constituting a simple and versatile tool for design.

Keywords: masonry infills, numerical modelling, parametric study, design model, strut-and-tie model.

1 – Associate Professor, University of Minho, Department of Civil Engineering, P-4800-058 Guimaraes, Portugal, E-mail: pbl@civil.uminho.pt; Phone: +351-253-510200; Fax: +351-253-510217

2 – Associate Professor, University Federal of Viçosa, Department of Civil Engineering – Viçosa – MG – Brazil, E-mail: ritadecassia@ufv.br; Phone: (+55) 3138991488; Fax: (+55) 3138991481

3 – Associate Professor, University Federal of Minas Gerais, Department of Structural Engineering – Belo Horizonte – MG – Brazil, E-mail: roberto@dees.ufmg.br; Phone: (+55) 3132381986.

1 INTRODUCTION

Masonry infill panels are usually present in steel and concrete framed structures. The masonry panels can be solid or with openings, even if, in most cases, they are considered as partition or enclosure walls, without any structural function. Such simplified procedure is, usually, excessively conservative, not economical and has several practical disadvantages for construction quality, namely: (a) damage in the partition walls because a low quality material is used and there is hardly a legal responsible for the building element; (b) insufficient detailing of masonry walls and masonry-frame connections; (c) severe damage and life losses in the case of earthquakes due to inadequate provisions. In fact, the interaction of the masonry infills with the surrounding frames has a major influence in the structural response of the full composite structure.

The masonry infill is very stiff and has considerable strength, meaning that the load capacity of masonry infilled frames increases substantially. In the case of horizontal loading due to wind or seismic action, it is usual to assume that an equivalent compression strut can replace the action of the masonry panels. This concept was introduced originally by Polyakov (1960) and further developed by Holmes (1961), Stafford-Smith (1966), Stafford-Smith and Carter (1969) and Riddington and Stafford-Smith (1978). In particular, the last two authors proposed simplified formulas and charts that take into account the width of the strut, the stiffness of the panel and frame, the geometric relations, the constitutive behaviour of masonry and the possible failure modes of the masonry panel. The concept was further extended to include three struts, with the aim of better reproducing the forces developed in beams and columns, e.g. El-Dakhkhni (2003).

The finite element method is the most popular analysis tool for complex structural engineering problems. The method suffered enormous developments in the recent decades related to the mathematical representation of the complex experimental behaviour and several

researchers analysed the behaviour of masonry infilled frames with this technique. Since the pioneer work of Mallick and Severn (1967), several difficulties were evident from the simulations, namely the issues of modelling the separation between frame and panel, of the bond strength and friction of the connection between frame and panel, and of the mechanical constitutive behaviour of masonry itself. Riddington and Stafford-Smith (1978) found that the critical stresses for the masonry panel are located in the centre and are mostly associated with tensile and shear failure. In this case, the frame-panel interaction was modelled by using double nodes and normal springs at the interfaces, with contact/separation modelled in a simplified way. King and Pandey (1978) further extended the numerical representation by adding interface elements capable of taking into account contact and friction for the frame-panel interaction. This work was further extended with non-linear behaviour of the panel and frame, by Liauw and Kwan (1982) and Dhanasekar and Page (1986) in the framework of continuum modelling, and by Mehrabi and Shing (1997) in the framework of discontinuum modelling.

Nevertheless, the usage of simplified rules in modern design of framed structures is unusual, partly due to the lack of a universally accepted theory and partly due to the fact that masonry is often considered today as a non-structural material. The present paper aims at providing a contribution for design based in a numerical parametric study and a simple strut-and-tie model. The model proposed is compared with the numerical and experimental results, and also with other simplified approaches.

2 BRIEF DESCRIPTION OF THE EXPERIMENTAL PROGRAM AND ADOPTED NUMERICAL SIMULATION

The experimental program was carried out in steel frames, infilled with masonry made using aerated autoclaved concrete blocks and glued joints with a polymeric mortar, see

Alvarenga (2002) for details. The frame was made using a steel profile with an I-section of $220 \times 200 \text{ mm}^2$. The masonry panels are made using blocks with dimensions $600 \times 300 \times 150 \text{ mm}^3$, with an average compressive strength of 4.5 N/mm^2 , and mortar with a strength of 8.9 N/mm^2 . The strength characteristics of masonry are a compressive strength of 2.6 N/mm^2 and a shear strength (racking test) of 0.17 N/mm^2 . Special care has been taken to ensure proper bond between the steel frame and the masonry panel, by pre-placement of a toothed layer of polymeric mortar around the complete frame in the day before building the infill. In addition, a 30 mm gap was left in the top of the panel, later filled with an expansive fluid mortar, so that full contact of between panel and frame was ensured.

Two different steel frames with one single bay were used with a relation between height and length equal to 0.83 e 0.51, see Fig. 1. Two specimens have been made for each h/l relation and other aspects, not addressed here, have been considered in the experimental program (mortar composition, dowels in frame-panel connection and openings), Alvarenga (2002). A monotonically increasing horizontal load was then applied to the frame until collapse of the panel. Before and after the tests, the frame was tested, confirming that the behaviour of the **steel frame** is fully elastic.

The typical results of the tests are shown in Fig. 2, in terms of failure patterns. Due to the very high bond of the polymeric mortar, the cracks cross units and joints in approximately straight lines. This is not in agreement with the typical stepped cracks observed in traditional masonry, built using strong units and weak mortars. The typical separation between frame and panel was nevertheless observed in several tests.

The finite element model adopted in the simulation was obviously prepared taking into account the observed behaviour. Given the discontinuous nature of failure, non-linear interface elements were adopted to represent the cracks, the interface between frame and panel and the steel connections, while non-linear continuum elements were used to represent

the masonry panel. The steel frame was kept linear elastic. The material model adopted for the interfaces is detailed in Lourenço et al. (1997) and for the continuum is detailed in Lourenço et al. (1998). The masonry tensile and compressive strength necessary for the analysis read $f_t = 0.26 \text{ N/mm}^2$ and $f_c = 2.6 \text{ N/mm}^2$, respectively. For details of the data required for the numerical simulations are given in Alvarenga (2002).

Fig. 3 illustrates the typical results of the numerical simulation, including deformed mesh and failure pattern, together with the compared load-displacement diagram. The separation between the steel frame and the masonry panel occurs very early because the bond is very weak. Afterwards, a first load drop is clear in the experiments, associated with the opening of the diagonal crack in the middle of the panel. This crack progresses almost instantaneously along the full size of the panel and leads to a small snap back in the numerical simulations (for a horizontal displacement of about 6 mm). In addition, it is also clear that the tests were stopped much before the final collapse load of the panel was reached as, in the numerical simulation, compressive failure of the masonry panel occurs in the corners at a much later stage. Nevertheless, for design purposes, it must be assumed that diagonal failure corresponds to the collapse load as the damage is not acceptable and requires costly repairs. In Alvarenga (2002), the experimental and numerical results are compared for all tested panels, in terms of failure load, failure pattern, length of frame-panel separation and deformation in the compressed masonry corners.

3 PARAMETRIC STUDY USING NUMERICAL MODELLING

In the experimental program only two different relations between height h and length l were considered. Moreover, the characteristics of the masonry panel and the steel frame were kept constant. Therefore, the experimental results are insufficient for the purpose of validating a simplified model for design. After the validation of the finite element simulation, a

parametric study was carried out taking into account: (a) different geometry; (b) different stiffness values for the steel frame connections; and (c) different stiffness ratio between steel frame and masonry panel.

3.1 Influence of the geometry of the panel

In order to evaluate the influence of the geometry in the response, the following relations between height h and length l have been considered: 0.51, 0.60, 0.70, 0.83 and 1.00. It is noted that the specimens tested experimentally had relations h / l equal to 0.51 and 0.83. The height of the masonry panel was kept constant and equal to 2.1 m, while the material parameters were kept constant in the analyses.

Fig. 4 illustrates the results obtained from the numerical simulations, in terms of force-displacement diagrams (only three diagrams are shown for the sake of keeping the clarity). It can be observed that the variation in the stiffness of the structure with the geometry is minor, both before and after diagonal cracking. This is due to the fact that the steel connections are rather flexible and the height of the structure is kept constant in the analysis. The failure mode is constant for all the analyses even if dramatic changes in the value of the cracking load are found (maximum of 308 kN and minimum of 138 kN, i.e. 55% variation). The cracking load decreases with increasing h/l ratio. The final collapse load due to crushing of the masonry corners is less sensitive to the geometry (maximum of 358 kN and minimum of 308 kN, i.e. 14% variation). The crushing load increases with increasing h/l ratio.

3.2 Influence of the connections stiffness

All the analyses presented in the previous section were repeated using different stiffness for the steel frame connections. The original analysis assumed semi-rigid connections, calibrated with experimental results obtained in the tests using the steel frame

alone. In addition, fixed and hinged connections are now assumed for the steel frame. Fig. 5 illustrates the numerical analysis typical results, in terms of load-displacement diagrams. It can be observed that the variation in the response of the structure with the stiffness of the frame connections is moderate, both before and mostly after diagonal cracking. This is due to the fact that the beam stiffness becomes more relevant for the global structural stiffness upon increasing stiffness of the connections. The failure mode is no longer constant for all the analyses because, in the case of h/l equal to 0.51 and a hinged frame, crushing in the corners occurs before diagonal cracking. It is also noted that the variation in the cracking load with the stiffness of the connection is low but the variation in the crushing load with the stiffness of the connection is moderate. This is evident from Fig. 6, which shows the cracking and crushing load for all analyses (with the single exception where crushing load occurred before cracking load, meaning that cracking of the panel is no longer possible). The crushing load decreases with increasing stiffness of the steel frame connections.

3.3 Influence of the stiffness ratio between steel frame and masonry panel

All the analyses presented regarding the influence of the geometry of the panel were repeated using different stiffness for the masonry panel, with the objective of assessing the influence of the ratio between the stiffness of the steel frame and the stiffness of masonry. The elasticity modulus of masonry was changed with respect to the original experimental E_0 value, by multiplying it by a factor equal to 0.5; 0.75; 1.0; 1.5; and 2.0. Fig. 7 illustrates typical results obtained from the numerical simulations, in terms of force-displacement diagrams (again only three diagrams are shown for the sake of keeping the clarity). The failure mode is also not constant for all the analyses and it can be observed that the variation in the stiffness of the structure with the connection stiffness is low before diagonal cracking

and moderate after diagonal cracking. It is also noted that the variation in the cracking load is significant but the variation in the crushing load is only moderate. This is evident from, which shows the cracking and crushing load for all analyses (with the single exception where crushing load occurred before cracking load, meaning that cracking of the panel is no longer possible). The cracking load decreases with increasing masonry stiffness, while the crushing load can both increase or decrease with increasing masonry stiffness.

4 PROPOSED DESIGN MODEL FOR MASONRY INFILLED FRAMES

From the failure modes observed in the tests and in the numerical simulations, the failure of masonry panels can be essentially attributed to diagonal cracking and corner crushing. In order to replicate such failures modes, the traditional equivalent single compression strut needs to be replaced by a slightly more complex strut-and-tie model (STM). STMs are limit analysis methods based on the plasticity theory, currently used in most reinforced concrete codes, e.g. Eurocode 2 (CEN, 2003). The reader is referred to Schlaich (1990) for details. It is noted that no reinforcement is present in the present case, but unidirectional tension fields can be defined and, at least, in the case of stepped diagonal cracks it is certain that masonry possesses some degree of plastic behaviour.

In case of masonry infilled frames subjected to horizontal loading the flow of internal loads is well known and the definition of an appropriate strut-and-tie model is straightforward. The compressive stresses form a strut oriented along the panel diagonal. The small contact between the frame and masonry panel leads to a fan in each panel corner, which might lead to diagonal cracking if the tensile strength of masonry is reached. Fig. 9 shows the load transfer mechanisms observed and the strut-and-tie model proposed, which consists of the replacement of a single equivalent strut by a set of four diagonal fanned struts and one tie normal to the equivalent strut. A horizontal force F is applied to the structure, leading to a

compression force in the strut given by $F/\cos\theta$, where θ is the angle of the panel diagonal defined with the horizontal. The contact length between the frame and the panel is assumed equal to α .

The forces in the compressed struts (C) and tensioned tie (T) can be obtained from the equilibrium of the nodes, leading to

$$C = \frac{F}{2 \times \cos \gamma \times \cos \theta} \quad (1)$$

$$T = \frac{F \times \tan \gamma}{\cos \theta} \quad (2)$$

where the angle between the struts is given by 2γ , with

$$\tan \gamma = \alpha \frac{\sqrt{2}}{2} \times \frac{\cos \theta}{l} \quad (3)$$

and l is equal to the length of the masonry panel.

4.1 Tensile failure check (diagonal cracking)

In order to obtain the tensile stress at the panel centre, a constant stress distribution is assumed in a central band equal to half the size of the diagonal, see Fig. 10a. The need to consider a smaller part of the equivalent strut is obvious from the experiments and numerical

simulation, as the corners are subjected to biaxial compression. The maximum tensile force T_{max} in the tie is then given by

$$T_{max} = \frac{f_t \times l \times t}{2 \cos \theta} \quad (4)$$

where f_t is the masonry tensile strength and t is equal to the width of the masonry panel. From Eq. (2), the maximum horizontal force F_{crack} that can be applied to the masonry infilled frame, leading to diagonal failure, is then given by

$$F_{crack} = \frac{f_t \times l \times t}{2 \tan \gamma} \quad (5)$$

4.2 Compressive failure check (corner crushing)

For the compressive failure check, only the corners are considered as the verification at the centre of the panel is less severe. At the corners, a triangular distribution of stresses is assumed in the contact zone between frame and panel, see Fig. 10b. Here, p_h and p_v are the maximum stress levels found in the contact length α , in the horizontal and vertical directions, respectively. The maximum stress level values are given by

$$p_h = \frac{2F}{\alpha \times t} \quad (6)$$

$$p_v = \frac{2F \times \tan \theta}{\alpha \times t} \quad (7)$$

Given the fact that the corners are subjected to biaxial compression, the maximum stress can be obtained in a simplified way by assuming an isotropic material (in the case of highly anisotropic masonry, a specific failure criterion must be adopted). Here, the expression from the Model Code 90 (CEB-FIP, 1992) is adopted, meaning that the maximum biaxial compressive strength is given by

$$f_c^{biax} = \frac{1 + 3.65 \times \tan \theta}{(1 + \tan \theta)^2} f_c \quad (8)$$

where f_c is the uniaxial compressive strength. Moreover, in the framework of limit analysis of concrete structures it is usual to adopt the concept of effective stress, which is a value lower than the uniaxial compressive strength that takes into account the load redistributions and the non-uniform distributions of stresses. The value for the effective stress f_c^* , Nielsen (1999), can be assumed equal to

$$f_c^* = \left[0.70 - \frac{f_c^*}{200} \right] \times f_c \quad \text{with } f_c \text{ in N/mm}^2 \quad (9)$$

Finally, from Eqs. (6-7), the maximum horizontal force F_{crush} that can be applied to the masonry infilled frame, leading to corner failure, is then given by

$$F_{crush} = \min \left\{ \begin{array}{l} \frac{f_c^{biax,*} \alpha t}{2} \\ \frac{f_c^{biax,*} \alpha t}{2 \tan \theta} \end{array} \right. \quad (10)$$

4.3 Influence of the frame connection stiffness

The parametric study carried out indicates that the force leading to corner failure of the infill, under compression, is directly proportional to the connection stiffness. As shown above, the rigid connection provides a horizontal force 35% larger than the hinged connection. On the contrary, the force leading to diagonal cracking does not exhibit considerable variation with the stiffness of the connection. Therefore, it is proposed that Eq. (10) is affected by a coefficient $(1+0.3\beta)$, given

$$F'_{crush} = (1 + 0.3\beta) F_{crush} \quad (11)$$

where β indicates the stiffness of the connection, such as $0 \leq \beta \leq 1$. For a hinged connection $\beta = 0$, for a semi-rigid connection ($0 < \beta < 1$) and for a rigid connection $\beta = 1$.

4.4 Definition of the contact length

The contact length between the frame and the panel was analysed in all numerical simulations, see Alvarenga (2002). The expressions proposed by Stafford-Smith and Carter (1969) fit reasonably well the values found numerically and can be used with the proposed model, given a contact length $\lambda L'$

$$\lambda L' = L' \times \sqrt[4]{\frac{E_{panel} t}{4E_p I_p h} \sin 2\theta} \quad (12)$$

$$\frac{\alpha}{L'} = \frac{\pi}{2\lambda \cdot L'} \quad (13)$$

where E_{panel} , t and h are the Young's modulus, thickness and height of the masonry panel, and E_p , I_p and L' are the Young's modulus, moment of inertia and length of the column (measured between the axes of the top and bottom beams), respectively.

5 VALIDATION OF THE PROPOSED DESIGN MODEL

In this section, the proposed simplified model is validated against the numerical parametric study and experimental results. The model is also compared with the predictions from the models from Stafford-Smith and Carter (1969) and Stafford-Smith and Riddington (1977).

Fig. 11 illustrates the results of the comparison between the numerical parametric study and the experimental results (it is noted that in the experiments, load application was stopped after diagonal cracking and crushing could not be found). For the proposed model, the value of the tensile strength f_t and the compressive strength f_c were the same as in the numerical simulations, as given above. The average error between the proposed model and the numerical simulations is equal to 14% (diagonal cracking) and 12% (corner crushing), which is rather acceptable for a simplified design model. Fig. 11 presents also a comparison with the simplified models of Stafford-Smith and Carter (1969), with an average error of 39% (diagonal cracking) and 24% (corner crushing), and Stafford-Smith and Riddington (1977), with an average error of 14% (diagonal cracking) and 23% (corner crushing). It can be observed that the proposed model provides better results.

As addressed in the previous section, crushing of the compressed corners is influenced by the stiffness of the beam-column connection. Fig. 12 presents the comparison between the

simplified model and the numerical parametric study for the different h / l ratios considered. The average error between the proposed model and the numerical simulations reads only 11%, which is again acceptable for a simplified design model.

The influence of the relation between the stiffness of the panel and the frame is analysed using Table 1. Even if moderate to large variations between the models and the parametric numerical study can be found, the average error for the proposed model is only 16%, which compares to an average error of 24% in Stafford-Smith and Carter (1969) and an average error of 20% in Stafford-Smith and Riddington (1977).

Finally, the proposed model is further compared with the experimental results from Braguim (1989). This author carried out twelve experimental tests in steel frames infilled with concrete block masonry. The masonry panel had dimensions of $3200 \times 2800 \text{ mm}^2$, with a modulus of elasticity of 5000 N/mm^2 , a compressive strength of 3.1 N/mm^2 , a tensile strength of 0.31 N/mm^2 and a thickness of 115 mm. The contact length calculated according to the proposal is 957 mm, for a relative stiffness parameter ($\lambda L'$) equal to 4.92. The values obtained from the proposal are 210.08 kN (diagonal cracking) and 242.48 kN (corner crushing), which compare to 174 / 167 kN and 217 / 217 kN for the tests, respectively. These results further validate the proposed design model.

6 CONCLUSIONS

The contribution of masonry panels for stiffness and strength of masonry infilled frames is significant. Nevertheless, their favourable effect is usually not taken into account because masonry partitions walls are assumed non-structural and reliable design tools are lacking.

In the present paper, advanced finite element simulations are validated from experimental results and, then, used to perform a parametric study on the response of masonry infilled frames. The parameters varied include the geometry, the stiffness of the steel frame connections and the relative stiffness between the steel frame and the masonry panel.

From the parametric study, a simplified model able to represent the collapse of masonry infills was proposed. The model is based on a decomposition of the usual diagonal strut in multiple struts and one tie. The proposed expressions for diagonal cracking and corner crushing are then compared with the parametric study and experimental results available in the literature, showing good agreement. The proposed tool is therefore a simple and useful approach for the design of masonry infilled panels.

ACKNOWLEDGEMENTS

The support by CAPES and UFV provided to the second author is gratefully acknowledged.

REFERENCES

Alvarenga, R.C.S.S. (2002), Experimental and theoretical analysis of composite structures of steel frames infilled with aerated autoclaved concrete masonry (in Portuguese), PhD thesis, University of São Paulo, School of Engineering from São Carlos, Brazil.

Available from www.civil.uminho.pt/masonry.

Braguim, J. R. (1989), Contributions to the study of stiffening in steel structures for high rise buildings (in Portuguese), MSc thesis, Polytechnic School, University of São Paulo, Brazil.

CEN (2004), Eurocode 2: Design of concrete structures – Part 1-1: General rules and rules for buildings, EN 1992-1-1, European Committee for Standardization, Brussels.

CEB-FIP (1993), Model Code 1990, Bulletin D'Information 213/214, Thomas Telford, London.

Dhanasekar, M., Page, A.W. (1986), The Influence of brick masonry infill properties on the behavior of infilled frames, *Proceedings of the Institution of Civil Engineers*, part 2, 81, 593-605.

El-Dakhakhni, W.W., Elgaaly, M., Hamid, A.A. (2003), Three-strut model for concrete masonry-infilled steel frames, *Journal of Structural Engineering*, ASCE, 129(2), 177-185.

Holmes, M. (1961), Steel Frames with Brickwork and Concrete Infilling. *Proc. Inst. Civ. Eng.*, 19, 473-478.

King, G.J.W., Pandey, P.C. (1978), The analysis of infilled frames using finite elements, *Proceedings of the Institution of Civil Engineers*, part 2, 65, 749-760.

Liauw, T.C., Kwan, K.H. (1982), Non-linear analysis of multi-storey infilled frames. *Proceedings of the Institution of Civil Engineers*, Part 2, 73, 441-454.

Lourenço, P.B., Rots, J.G. (1997), A multi-surface interface model for the analysis of masonry structures, *Journal of Engineering Mechanics*, ASCE, 123(7), 660-668.

Lourenço, P.B., Rots, J.G., Blaauwendraad, J. (1998), Continuum model for masonry: Parameter estimation and validation, *Journal of Structural Engineering*, ASCE, 124(6), 642-652.

Mehrabi, A.B., Shing, P.B. (1997), Finite element modelling of masonry-infilled RC frames, *Journal of Structural Engineering*, ASCE, 123(5), 604-613.

Mallick, D.V., Severn, R.T. (1967), The behaviour of infilled frames under static loading, *Proceedings of the Institution of Civil Engineers*, 38, 639-656

Nielsen, M. (1999), Limit analysis and concrete plasticity, 2nd edition, CRC Press.

Polyakov, S.V. (1960), On the interaction between masonry filler walls and enclosing frame when loaded in the plane of the wall, in "Earthquake Engineering", Earthquake Engineering Research Institute, San Francisco, 36-42.

Riddington, J.R., Stafford-Smith, B. (1978), Composite method of design for heavily loaded wall-beam structures, *Proceedings of the Institution of Civil Engineers*, Part 1, 64, 137-151.

Schlaich, J. (1990), Toward a consistent design of structural concrete, *PCI Journal*, 32(3), 74-150.

Stafford-Smith, B. (1966), Behaviour of square infilled frames, *Journal of the Structural Division*, ASCE, 92(ST1), 381-403.

Stafford-Smith, B., Carter, C. (1969), A method of analysis for infilled frames. *Proceedings of the Institution of Civil Engineers*, 44, 31-48.

Stafford-Smith, B., Riddington, J. R. (1977). Analysis of infilled frames subject to racking with design recommendations. *The Structural Engineer*, 6(55), 263-268.

LIST OF FIGURES

Fig. 1 – Masonry infilled frames used in the experimental program, using a relation between height h and length l equal to: (a) $h / l = 0.83$; (b) $h / l = 0.51$

Fig. 2 – Typical experimental failure patterns: (a) $h / l = 0.83$; (b) $h / l = 0.51$

Fig. 3 – Typical results of the numerical simulation (panel with $h / l = 0.83$): (a) deformed mesh with separation between frame and panel, and with cracked panel; (b) horizontal load-displacement diagrams

Fig. 4 – Selected results of the numerical simulation for different panel geometry

Fig. 5 – Typical results of the numerical simulation for different connection stiffness ($l/h = 0.51$)

Fig. 6 – Influence of the geometry and connection stiffness: (a) cracking load; (b) crushing load

Fig. 7 – Typical results of the numerical simulation for different masonry stiffness ($l/h = 1.00$)

Fig. 8 – Influence of the geometry and masonry stiffness: (a) cracking load; (b) crushing load

Fig. 9 – Design model for masonry infill subjected to a horizontal load F : (a) composite frame-panel; (b) proposed strut-and-tie model

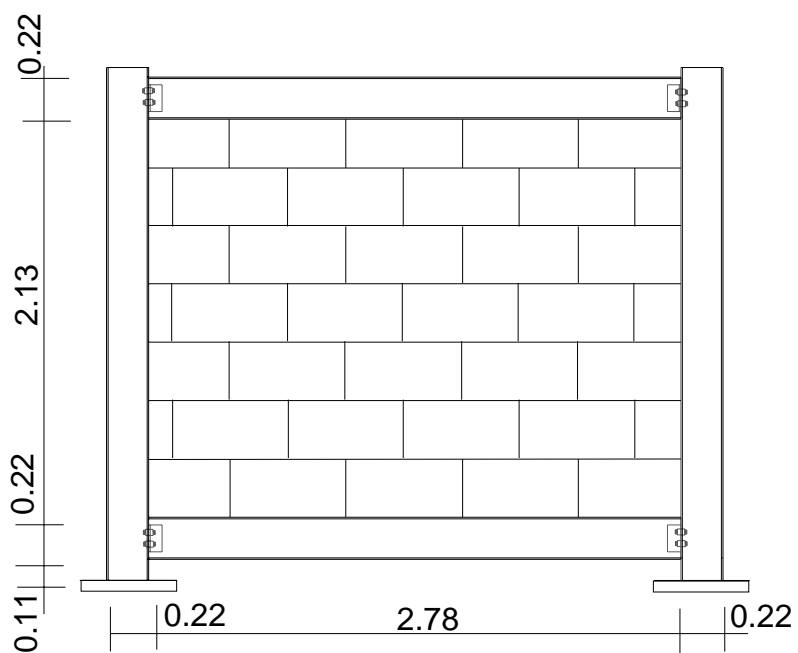
Fig. 10 – Safety checks for the strut-and-tie model: (a) tensile check for diagonal cracking; (b) compressive check for corner crushing

Fig. 11 – Comparative analysis between the results obtained for the different h / l ratio: (a) force leading to cracking of the diagonal; (b) force leading to crushing of the compressed corner

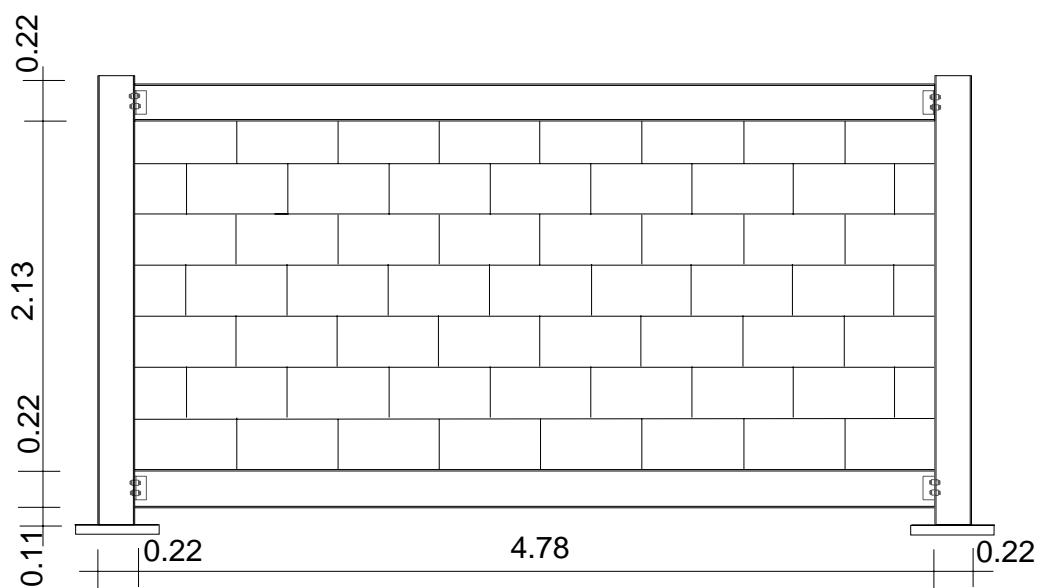
Fig. 12 – Comparative analysis between the results obtained for the force leading to crushing of the compressed corner, in the case of different h / l ratios and different connection stiffness (_M indicates the proposed model and _A indicates the numerical analysis)

LIST OF TABLES

Table 1 – Comparative analysis between the results obtained for the force leading to diagonal cracking and crushing of the compressed corner, in the case of different h / l ratios and different stiffness values for the masonry panel (n/a indicates that the failure mode did not occur in the numerical analysis)

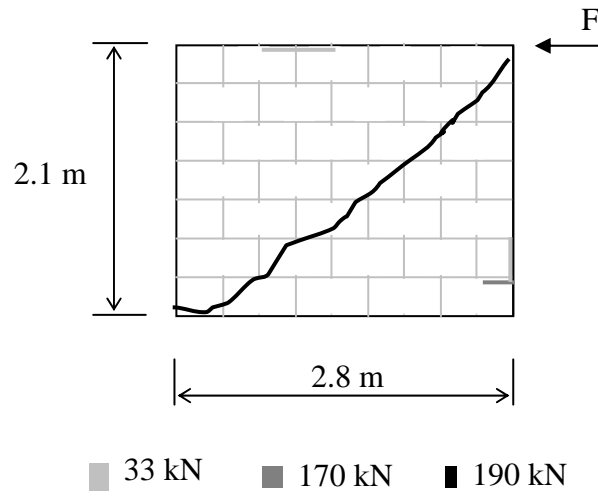


(a)

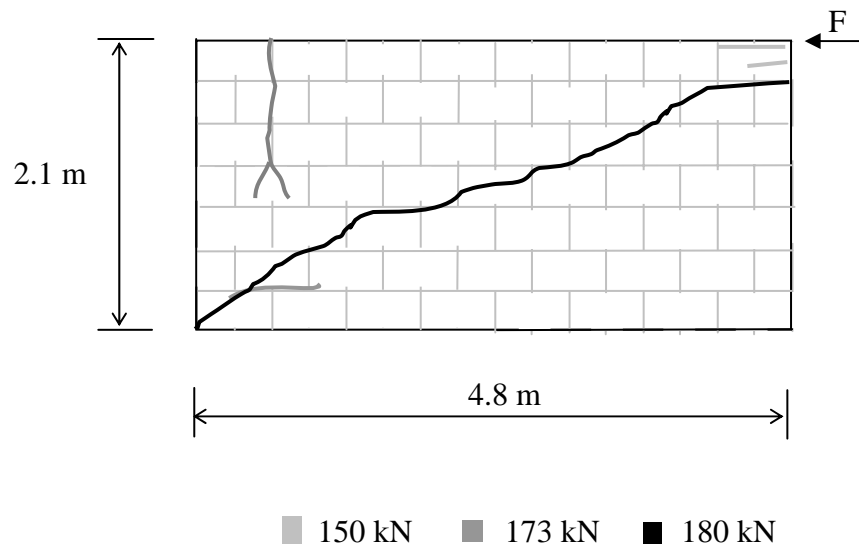


(b)

Fig. 1 – Masonry infilled frames used in the experimental program, using a relation between height h and length l equal to: (a) $h/l = 0.83$; (b) $h/l = 0.51$

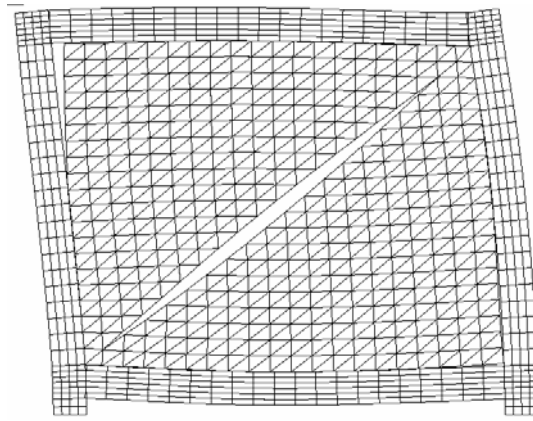


(a)

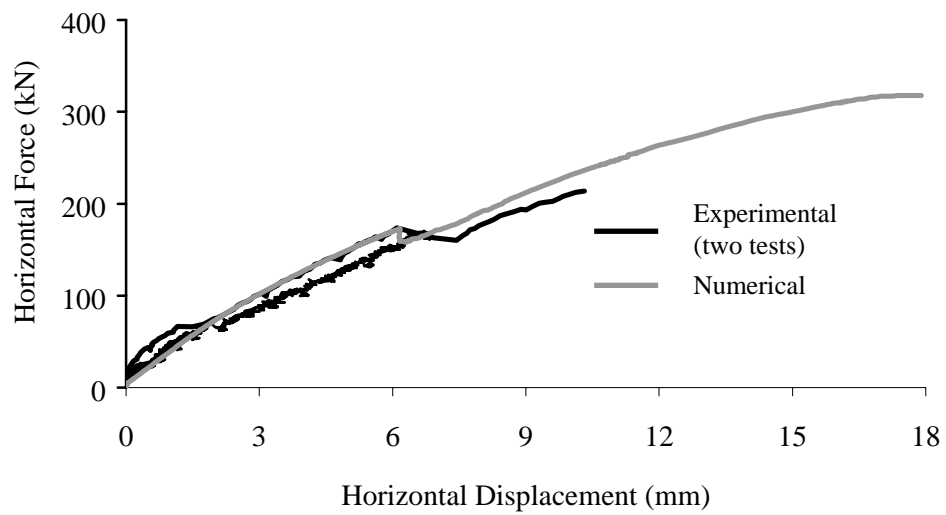


(b)

Fig. 2 – Typical experimental failure patterns: (a) $h/l = 0.83$; (b) $h/l = 0.51$



(a)



(b)

Fig. 3 – Typical results of the numerical simulation (panel with $h / l = 0.83$): (a) deformed mesh with separation between frame and panel, and with cracked panel;
(b) horizontal load-displacement diagrams

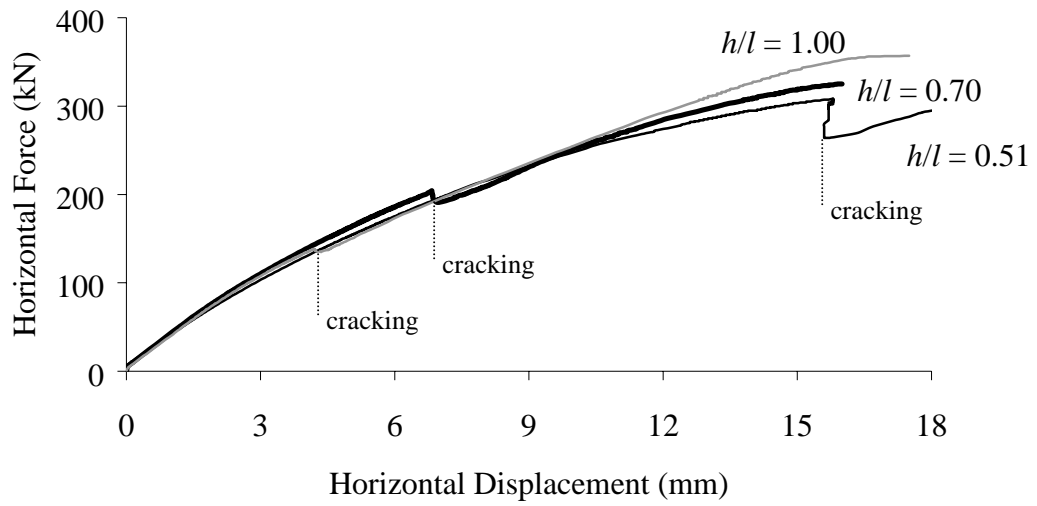


Fig. 4 – Selected results of the numerical simulation for different panel geometry

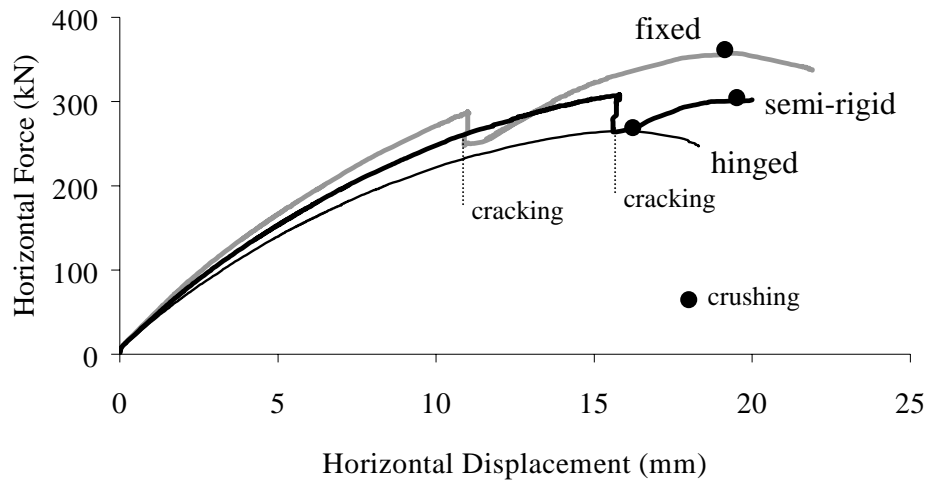
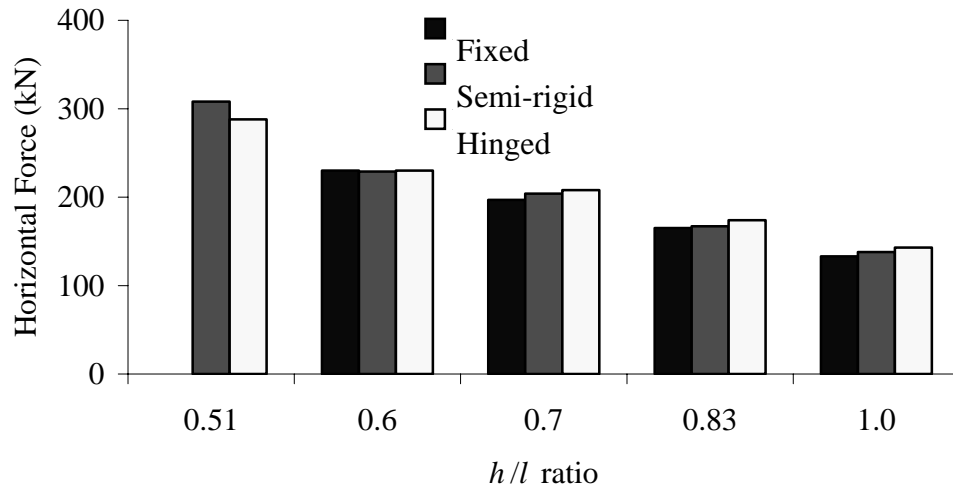
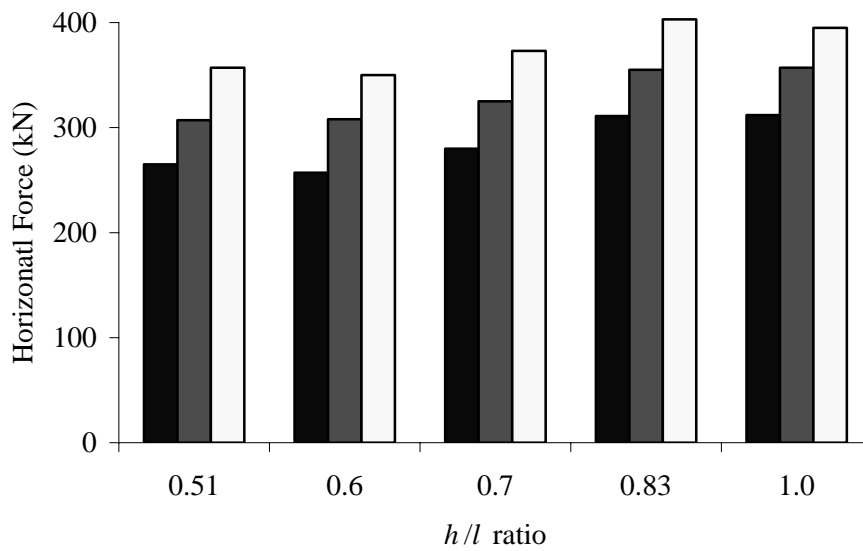


Fig. 5 – Typical results of the numerical simulation for different connection stiffness ($l/h = 0.51$)



(a)



(b)

Fig. 6 – Influence of the geometry and connection stiffness: (a) cracking load; (b) crushing load

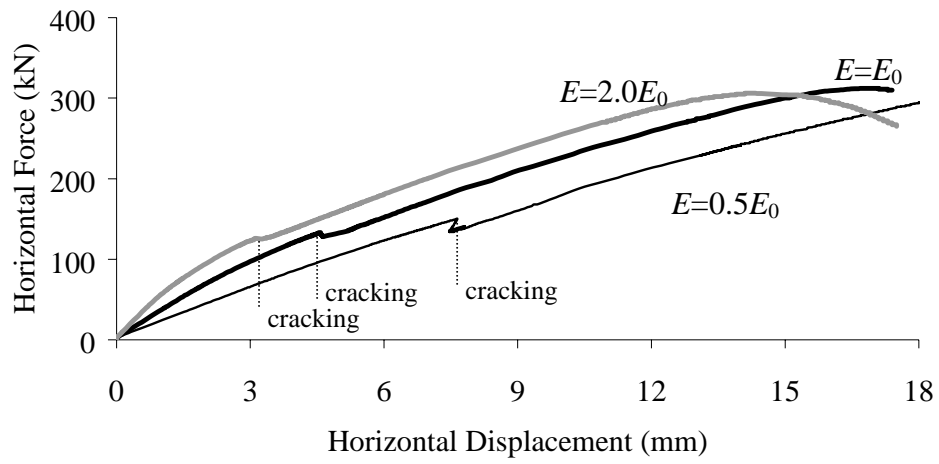
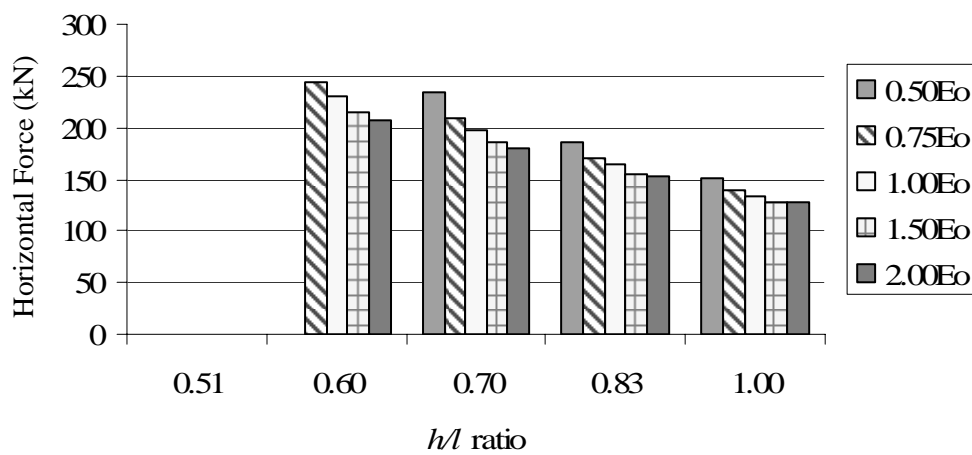
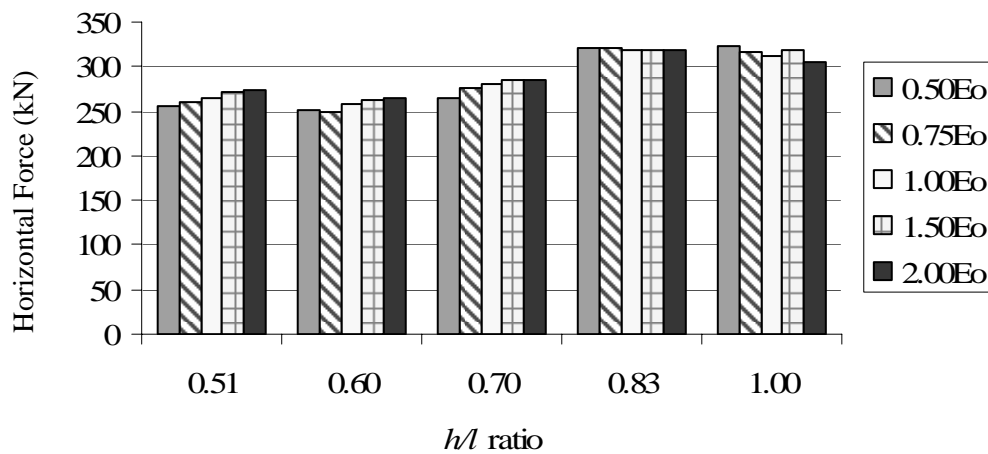


Fig. 7 – Typical results of the numerical simulation for different masonry stiffness ($l/h = 1.00$)

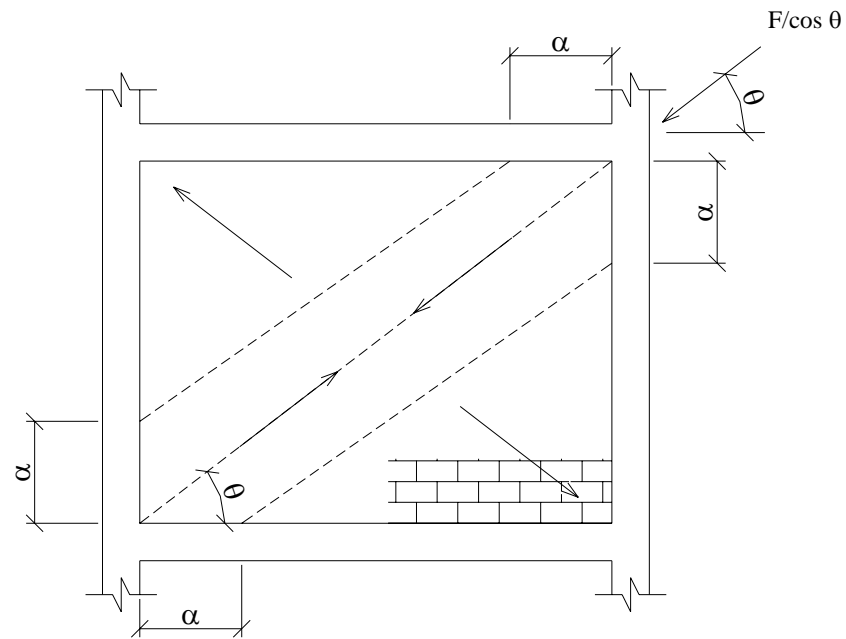


(a)

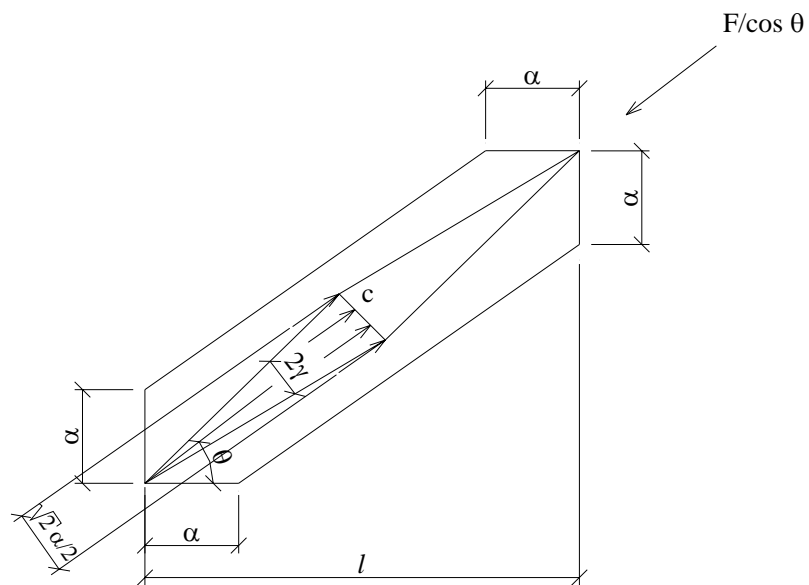


(b)

Fig. 8 – Influence of the geometry and masonry stiffness: (a) cracking load; (b) crushing load

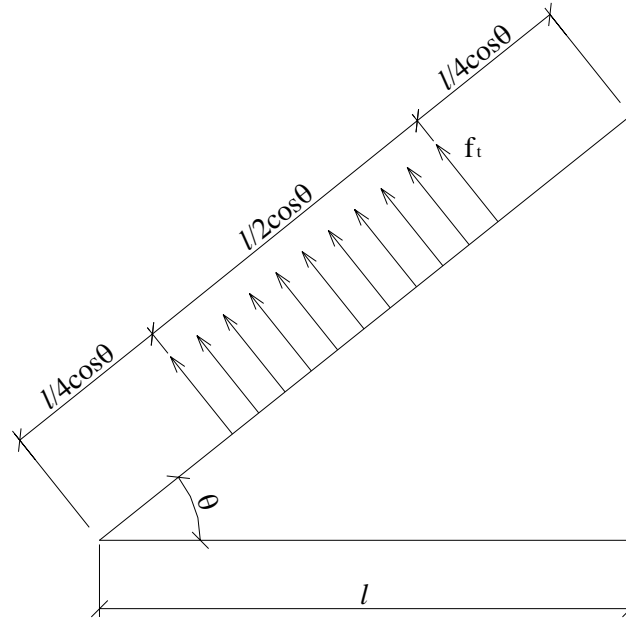


(a)

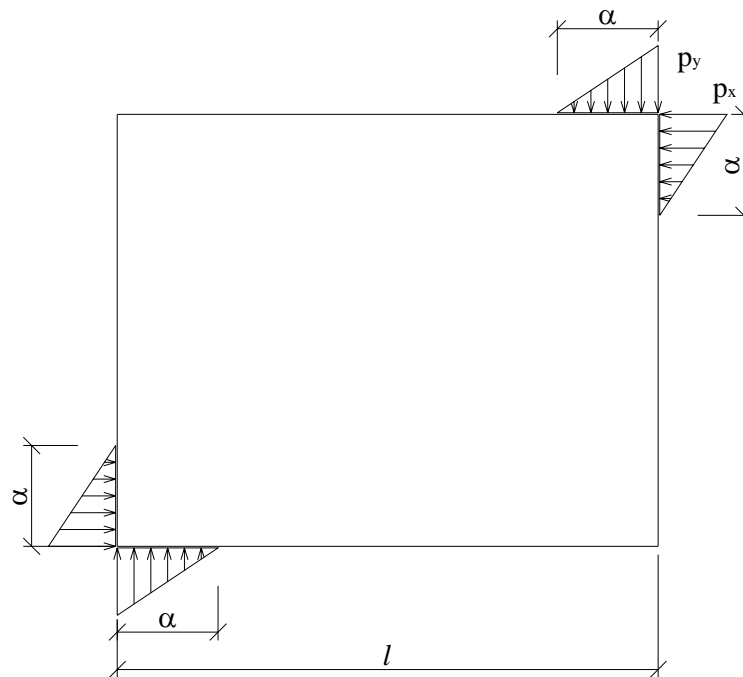


(b)

Fig. 9 – Design model for masonry infill subjected to a horizontal load F : (a) composite frame-panel; (b) proposed strut-and-tie model



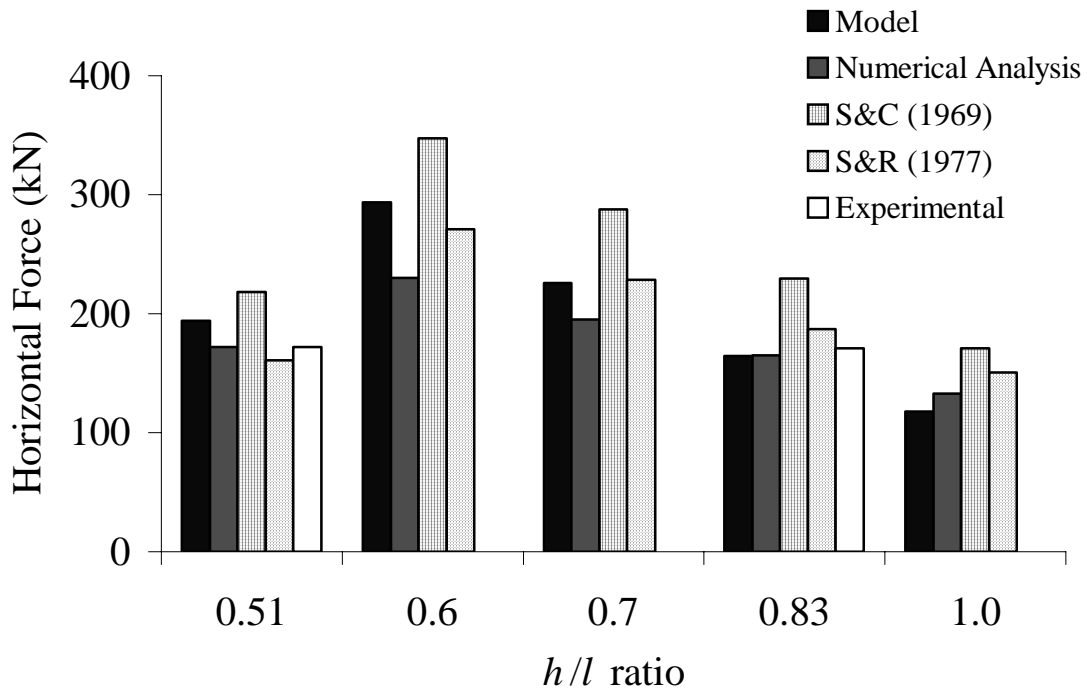
(a)



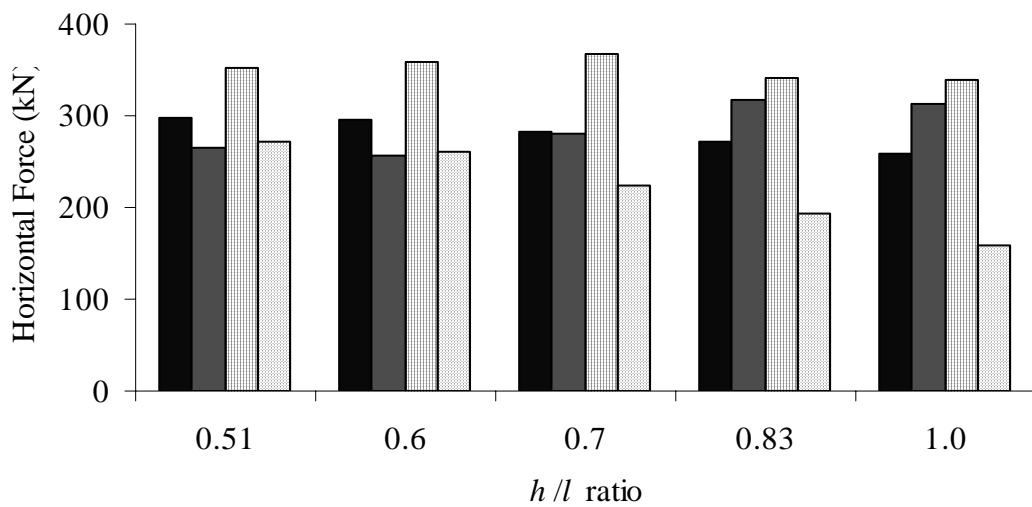
(b)

Fig. 10 – Safety checks for the strut-and-tie model: (a) tensile check for diagonal cracking;

(b) compressive check for corner crushing



(a)



(b)

Fig. 11 – Comparative analysis between the results obtained for the different h / l ratio:

(a) force leading to cracking of the diagonal; (b) force leading to crushing of the compressed corner

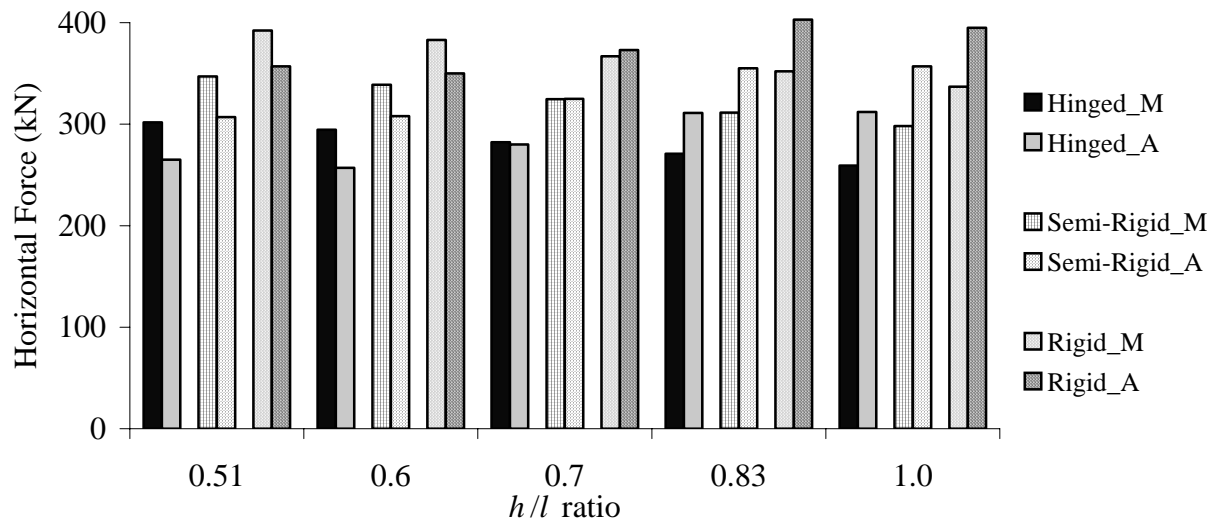


Fig. 12 – Comparative analysis between the results obtained for the force leading to crushing of the compressed corner, in the case of different h / l ratios and different connection stiffness (_M indicates the proposed model and _A indicates the numerical analysis)

Table 1 – Comparative analysis between the results obtained for the force leading to diagonal cracking and crushing of the compressed corner, in the case of different h / l ratios and different stiffness values for the masonry panel (n/a indicates that the failure mode did not occur in the numerical analysis)

			H / l ratio				
			0.51	0.6	0.7	0.83	1.0
E = 875	Diagonal cracking	Model	332.7	247.0	190.3	138.2	99.1
		Analysis	n/a	n/a	234.0	185.0	150.0
		S&C (1969)	408.3	356.7	292.9	234.2	173.1
		S&R (1977)	321.4	271.0	228.6	186.9	150.6
	Corner crushing	Model	355.0	256.0	410.8	314.7	355.1
		Analysis	350.3	251.0	379.8	304.5	350.3
		S&C (1969)	334.6	264.0	416.5	260.2	334.6
		S&R (1977)	322.1	320.0	406.0	224.9	322.1
E = 1312.5	Diagonal cracking	Model	368.2	273.3	210.6	153.0	109.7
		Analysis	n/a	243.0	209.0	171.0	139.0
		S&C (1969)	443.1	356.7	290.4	231.8	173.1
		S&R (1977)	321.4	271.0	228.6	186.9	150.6
	Corner crushing	Model	320.8	316.6	302.4	291.0	278.5
		Analysis	261.0	250.0	276.0	321.0	316.0
		S&C (1969)	376.9	371.5	377.1	370.3	352.8
		S&R (1977)	288.4	278.6	238.1	205.6	170.0
E = 1750	Diagonal cracking	Model	395.2	293.7	225.6	164.4	117.9
		Analysis	n/a	230.0	195.0	165.0	133.0
		S&C (1969)	436.4	347.5	287.9	229.5	170.9
		S&R (1977)	321.4	271.0	228.6	186.9	150.6
	Corner	Model	298.9	294.6	282.2	270.8	259.2

	crushing	Analysis	265.0	257.0	280.0	318.0	312.0
		S&C (1969)	352.7	359.2	366.6	342.0	338.2
		S&R (1977)	270.7	261.7	223.0	192.7	159.4
E = 2625	Diagonal cracking	Model	437.8	325.1	250.4	181.9	130.5
		Analysis	n/a	215.0	186.0	155.0	127.0
		S&C (1969)	428.2	347.5	279.1	227.1	167.7
		S&R (1977)	321.4	271.0	228.6	186.9	150.6
	Corner crushing	Model	269.8	266.2	254.3	244.7	234.2
		Analysis	271.0	263.0	284.0	319.0	319.0
		S&C (1969)	330.0	325.0	318.0	311.3	303.4
		S&R (1977)	247.2	239.2	242.0	176.6	172.2
E = 3500	Diagonal cracking	Model	251.1	247.7	236.6	227.7	218.0
		Analysis	274.0	265.0	286.0	318.0	306.0
		S&C (1969)	314.5	298.8	295.6	291.6	290.0
		S&R (1977)	232.2	224.8	191.8	165.5	137.0
	Corner crushing	Model	251.1	247.7	236.6	227.7	218.0
		Analysis	274.0	265.0	286.0	318.0	306.0
		S&C (1969)	314.5	298.8	295.6	291.6	290.0
		S&R (1977)	232.2	224.8	191.8	165.5	137.0